

RELATIVISTIC FIELD-THEORETICAL FORMULATION OF THE  
THREE-DIMENSIONAL EQUATIONS FOR THE THREE FERMION SYSTEM

A. I. MACHAVARIANI

*Joint Institute for Nuclear Research, Moscow Region, 141980 Dubna, Russia*  
*High Energy Physics Institute of Tbilisi State University, University Str. 9, 380086*  
*Tbilisi, Georgia*

Received 30 October 2003; Accepted 30 October 2004  
Online 22 November 2004

A new kind of the relativistic equations for the three-fermion systems are suggested. These equations are derived in the framework of the standard field-theoretical  $S$ -matrix approach in the time-ordered three-dimensional form. Therefore the corresponding relativistic covariant equations are three-dimensional from the beginning and the considered formulation is free of the ambiguities which appear due to a three-dimensional reduction of the four-dimensional Bethe–Salpeter equations. The solutions of the considered equations satisfy automatically the unitarity condition, and for the leptons, these equations are exactly gauge invariant even after the truncation over the multiparticle ( $n > 3$ ) intermediate states. Moreover, the form of these three-body equations does not depend on the choice of the model Lagrangian and it is the same for the formulations with and without quark degrees of freedom. The effective potential of the suggested equations is defined by the vertex functions with two on-mass shell particles. It is emphasized that these INPUT vertex functions can be constructed from experimental data. Special attention is given to the comparison with the three-body Faddeev equations. Unlike these equations, the suggested three-body equations have the form of the Lippmann–Schwinger–type equations with the connected potential. In addition, the microscopical potential of the suggested equations contains the contributions from the three-body forces and from the particle creation (annihilation) mechanism on the external particles. The structure of the three-body forces, appearing in the considered field-theoretical formulation, is analyzed.

PACS numbers: 11.80.-a, 11.80.-m, 11.10-z, 25.80.Hp, 21.45.+ , 24.10.Jv UDC 539.128.3  
Keywords: three-fermion systems, relativistic equations, Faddeev equations, Lippmann–Schwinger–type equations

## 1. Introduction

The purpose of this paper is to focus on the three-body equations with the particle creation and annihilation phenomena. The most popular tool for this in-

vestigation is the three-body generalization of the Bethe-Salpeter equations [1,2]. Unfortunately, in this four-dimensional formulation arises a set of complications which require the use of some serious approximations. For instance, due to the three-dimensional reduction of the four-dimensional Bethe-Salpeter equations arise the ambiguities regarding the choice of the form of the three-dimensional Green functions and the three-dimensional effective potentials. Next, the difficulties with the unitarity and the gauge invariance require the use of the tree approximation for the effective potentials and the one-particle propagators for the practical calculation. In addition, the potential of the Bethe-Salpeter equation is constructed through the three-variable vertex functions, which are required as the “input” functions. Therefore, in the calculations based on the Bethe-Salpeter equations or their quasipotential reductions, the off-mass shell variables in the vertex functions are usually neglected or a separable form for all three variables is introduced.

We consider another way of derivation of the three-body field-theoretical equations which allows to avoid the above difficulties and which can be solved with a considerably smaller number of approximations. The organization of this paper is as follows. First I consider the three-body spectral decomposition equations (which have the form of the off shell unitarity conditions [3,4]) for the amplitudes of the three-fermion systems. These equations form a base for the derivation of the Lippmann–Schwinger type equation [3,4]. After separation of the connected and disconnected parts in the amplitudes and effective potentials in these three-body spectral decomposition equations, one can separate the three-body equations for the connected and disconnected parts in the three-body amplitudes. Next, after linearization of these three-body equations we will get the three-body Lippmann–Schwinger equations for the connected part of the three-body amplitudes. The major difference between these equations and the Faddeev equations will also be discussed. Afterwards, I consider the structure of the three-body potentials for the three-fermion (three-electron or three-nucleon, or for the electron-deuteron scattering, etc.) systems. Finally, a short summary will be presented.

## 2. *The three-body Lippmann–Schwinger type equations for the three-fermion scattering reactions*

The problem of the relativistic description of particle interactions in the framework of a potential picture is usually solved by relativistic generalization of the Lippmann–Schwinger type equation of the nonrelativistic collision theory [3,4]. As the basis for the derivation of the Lippmann–Schwinger type equations in the collision theory, one can use the following quadratically nonlinear integral equations [4]

$$\begin{aligned}
 T_{\alpha\beta}(E_\beta) = & V_{\alpha\beta} + \sum_{\gamma} T_{\alpha\gamma}(E_\gamma) \frac{1}{E_\beta - E_\gamma + i\epsilon} T_{\beta\gamma}^*(E_\gamma) \\
 & + \sum_{d3} T_{\alpha,d3}(E_{d3}) \frac{1}{E_\beta - E_{d3}} T_{\beta,d3}^*(E_{d3}), \quad (1)
 \end{aligned}$$

where  $T_{\alpha\beta}(E_\beta)$  is the transition amplitude between the channels  $\alpha$  and  $\beta$ . The  $\alpha, \beta, \gamma$  denote the pure three noninteracting fermion channels or the one-fermion + two-body cluster states. For example, for the three nucleon systems  $\alpha = \text{NNN}$  or  $\text{Nd}$ , for the two-electron and nucleon  $\alpha = \text{eeN}$  or  $\text{ed}$  etc.,  $d3$  relates to the three-body bound states.  $\sum_\gamma$  stands for the integration over the momenta and the summation over the quantum numbers of the complete set intermediate  $\gamma \equiv |\gamma\rangle$ -channel states.

If we suppose, that there exists the full hermitian Hamiltonian  $H$  which has the complete set of the eigenfunctions  $H|\Psi_\gamma\rangle = E_\gamma|\Psi_\gamma\rangle$ , then one can easily reduce Eq. (1) to the Lippmann–Schwinger type equations

$$T_{\alpha\beta}(E_\beta) = V_{\alpha\beta} + \sum_\gamma V_{\alpha\gamma} \frac{1}{E_\beta - E_\gamma + i\epsilon} T_{\gamma\beta}(E_\beta), \quad (2)$$

where we have used the decomposition formula of the full Green function  $G(E) = 1/(E - H + i\epsilon)$  over the complete set of the functions  $|\Psi_\gamma\rangle$ , and we have taken into account the connection formula between an amplitude, a multichannel potential and a wave function  $T_{\alpha\beta}(E_\beta) = \langle\alpha|V|\Psi_\beta\rangle$  [3,4].

The three-body equations (1) are well defined after separation of the connected ( $T_{\alpha\beta}^c; V_{\alpha\beta}^c$ ) and disconnected ( $V_{\alpha\beta}^{dc}; T_{\alpha\beta}^{dc}$ ) parts of amplitudes and potentials. Therefore we split the complete amplitude and the complete potential in Eq. (1) into two corresponding parts

$$V_{\alpha\beta} = V_{\alpha\beta}^c + V_{\alpha\beta}^{dc}, \quad \text{and} \quad T_{\alpha\beta}(E_\beta) = T_{\alpha\beta}^c(E_\beta) + T_{\alpha\beta}^{dc}(E_\beta). \quad (3)$$

The disconnected parts of the two-body and three-body amplitudes are depicted in Fig. 1. The disconnected part of the three-body amplitudes is independent from the connected part of these amplitudes, because the two-body clusters with the asymptotic free third particle is independent of the three-particle interacted clusters. This is the usual requirement for the independence of the asymptotic clusters. The independence of the equations for the disconnected part of Eq. (1) can be easily demonstrated in the quantum-field formulation [8]. As a result, Eq. (1) is split into two sets of independent equations

$$T_{\alpha\beta}^{dc}(E_\beta) = V_{\alpha\beta}^{dc} + \sum_\gamma T_{\alpha\gamma}^{dc}(E_\gamma) \frac{1}{E_\beta - E_\gamma + i\epsilon} [T_{\beta\gamma}^{dc}(E_\gamma)]^*, \quad (4)$$

$$T_{\alpha\beta}^c(E_\beta) = W_{\alpha\beta} + \sum_\gamma T_{\alpha\gamma}^c(E_\gamma) \frac{1}{E_\beta - E_\gamma + i\epsilon} [T_{\beta\gamma}^c(E_\gamma)]^* + \sum_{d3} T_{\alpha,d3}(E_{d3}) \frac{1}{E_\beta - E_{d3}} T_{\beta,d3}^*(E_{d3}), \quad (5)$$

where

$$W_{\alpha\beta} = V_{\alpha\beta}^c + \sum_\gamma T_{\alpha\gamma}^c(E_\gamma) \frac{1}{E_\beta - E_\gamma + i\epsilon} [T_{\beta\gamma}^{dc}(E_\gamma)]^* + \sum_\gamma T_{\alpha\gamma}^{dc}(E_\gamma) \frac{1}{E_\beta - E_\gamma + i\epsilon} [T_{\beta\gamma}^c(E_\gamma)]^*. \quad (6)$$

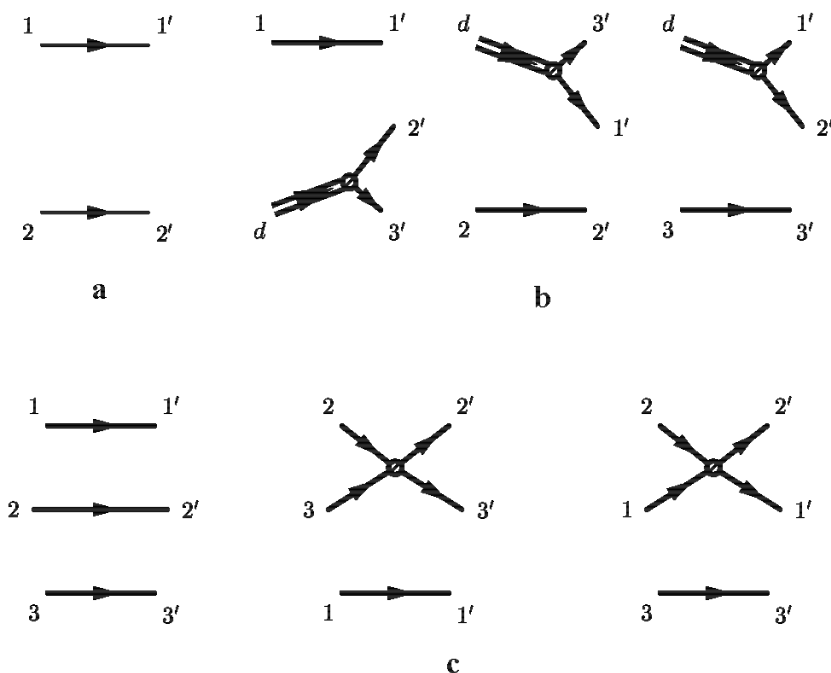


Fig. 1. The disconnected parts of the two-fermion and the three-fermion  $S$ -matrix elements. The label  $d$  stands for the two-fermion bound state. The shaded circle corresponds to the two-body scattering amplitude.

The effective potential (6) in the field-theoretical formulation  $w_{\alpha,\beta}$  is not hermitian due to the particle propagators in the intermediate states. Nevertheless, we have shown in Refs. [8] and [11] that the quadratically nonlinear equations (5) are equivalent to the following Lippmann–Schwinger type equations

$$\mathcal{T}_{\alpha\beta}(E_\beta) = U_{\alpha\beta}(E_\beta) + \sum_{\gamma} U_{\alpha\gamma}(E_\beta) \frac{1}{E_\beta - E_\gamma + i\epsilon} \mathcal{T}_{\gamma\beta}(E_\beta), \quad (7)$$

where, for the sake of simplicity in above equations, we have omitted the delta function for the total three-momentum conservation,  $(2\pi)^3 \delta(\mathbf{P}_\beta - \mathbf{P}_\gamma)$ . The explicit form of the linear energy depending potential

$$U_{\alpha\beta}(E) = A_{\alpha\beta} + E B_{\alpha\beta}, \quad (8a)$$

with hermitian matrices  $A$  and  $B$

$$A_{\alpha\beta} = A_{\beta\alpha}^*, \quad B_{\alpha\beta} = B_{\beta\alpha}^* \quad (8b)$$

is considered in the next section.  $U_{\alpha\beta}(E)$  is simply connected with the  $W_{\alpha\beta}$ -potential (6)

$$U_{\alpha\beta}(E_\alpha) = W_{\alpha\beta}. \quad (9a)$$

Therefore, for any potential  $W_{\alpha\beta}$ , one can unambiguously construct  $U_{\alpha\beta}(E)$ . Solutions of equations (5) and (7) coincide on the energy shell

$$\mathcal{T}_{\alpha\beta}(E_\beta = E_\alpha) = T_{\alpha\beta}^c|_{E_\beta=E_\alpha}, \tag{9b}$$

and in the half on energy shell region, these amplitudes are simply connected

$$\mathcal{T}_{\alpha\beta} = W_{\alpha\beta} + \sum_\gamma W_{\alpha\gamma} \frac{1}{E_\beta - E_\gamma + i\epsilon} T_{\gamma\beta}^c(E_\beta). \tag{10}$$

The Lippmann–Schwinger type equations (7) are our final equations for the three-fermion scattering amplitudes. On the other hand, Eq. (1) can be linearized without the separation of the connected and disconnected parts, and from the Lippmann–Schwinger equation (2), one can derive the Faddeev type equations [3]. The advantage of Eq. (7) is that it does not need the splitting into four pieces  $V_{\alpha\beta} = \sum_{i=1}^3 V_{\alpha\beta}^i + V_{\alpha\beta}^c$  in order to take into account the disconnected parts in the perturbation series. Besides, Eqs. (7) are free from the over-counting problem which appears due to special disconnected diagrams and which generates the corresponding modification of the effective potentials [1,2].

### 3. The three-dimensional three-body field-theoretical equations

In the standard formulation of the quantum field theory [5–7], the  $S$ -matrix element between the asymptotic three-body states  $\alpha = 1', 2', 3', f'd'$  and  $\beta = 1, 2, 3, fd$  is connected by the scattering amplitude  $f_{\alpha,\beta}$

$$S_{\alpha,\beta} = \langle \text{out}; \alpha | \beta; \text{in} \rangle = \langle \text{out}; \tilde{\alpha} | b_{\mathbf{p}_a}(\text{in}) | \tilde{\beta}; \text{in} \rangle - (2\pi)^4 i \delta^{(4)}(P_\alpha - P_\beta) f_{\alpha,\beta}, \tag{11}$$

where  $f$  denotes the one-fermion state,  $d$  stands for the bound state of two fermions,  $P_\alpha \equiv (E_\alpha, \mathbf{P}_\alpha)$  is the complete four-momentum of the asymptotic state  $\alpha$ ,  $a$  and  $b$  corresponds to the one-fermion states extracted from the asymptotic  $\alpha$  and  $\beta$  states

$$\alpha = a + \tilde{\alpha}, \quad \beta = b + \tilde{\beta}, \tag{12}$$

and the four-momentum of the asymptotic one-fermion states  $a$  is  $p_a = (\sqrt{m_a^2 + \mathbf{p}_a^2}, \mathbf{p}_a) \equiv (E_{\mathbf{p}_a}, \mathbf{p}_a)$ . The amplitude  $f_{\alpha\beta}$  has the form

$$f_{\alpha\beta} = -\langle \text{out}; \tilde{\alpha} | J_{\mathbf{p}_a}(0) | \beta; \text{in} \rangle, \tag{13}$$

where  $J_{\mathbf{p}_a}(x)$  is the current operator of the fermion  $a$  which is determined by the Dirac equation  $J_{\mathbf{p}_a}(x) = Z_a^{-1/2} \bar{u}(\mathbf{p}_a)(i\gamma_\mu \partial_x^\mu - m_a)\psi_a(x)$  with the renormalization constant  $Z_a$  and Dirac bispinor function  $u(\mathbf{p}_a)$  [5,6].

Using the well know reduction formulas, we obtain

$$\begin{aligned}
 f_{\alpha\beta} &= \langle \text{out}; \tilde{\alpha} | b_{\mathbf{p}_b}^+ (\text{out}) J_{\mathbf{p}_a} (0) | \tilde{\beta}; \text{in} \rangle - \langle \text{out}; \tilde{\alpha} | \left\{ J_{\mathbf{p}_a} (0), b_{\mathbf{p}_b}^+ (0) \right\} | \tilde{\beta}; \text{in} \rangle \\
 &+ i \int d^4x e^{-ip_b x} \langle \text{out}; \tilde{\alpha} | T \left( J_{\mathbf{p}_a} (0) \bar{J}_{\mathbf{p}_b} (x) \right) | \tilde{\beta}; \text{in} \rangle, \quad (14)
 \end{aligned}$$

where

$$b_{\mathbf{p}_b}^+ (x_0) = Z_b^{-1/2} \int d^3x e^{-ip_b x} \bar{u}(\mathbf{p}_b) \gamma_0 \psi_b(x). \quad (15)$$

Here and afterwards, we use the definitions and normalization conditions from the Itzykson and Zuber's book [6].

After the substitution of the complete set of the asymptotic "in" states  $\sum_n |n; \text{in}\rangle \langle \text{in}; n| = \hat{1}$  between the current operators in expression (14), and after integration over  $x$ , we get

$$f_{\alpha\beta} = W_{\alpha\beta} + (2\pi)^3 \sum_{\gamma} f_{\alpha\gamma} \frac{\delta^{(3)}(\mathbf{p}_b + \mathbf{P}_{\tilde{\beta}} - \mathbf{P}_{\gamma})}{E_{\mathbf{p}_b} + P_{\tilde{\beta}}^0 - P_{\gamma}^0 + i\epsilon} \mathcal{T}_{\beta\gamma}^* \quad (16)$$

where  $W_{\alpha\beta}$  contains all contributions from intermediate states that can appear in the  $\beta \rightarrow \alpha$  reaction, except the  $s$ -channel three-particle  $\gamma = 1''2''3''$  exchange states and one-fermion  $f$  + two-fermion bound states  $d$  ( $\gamma = f + d$ ) exchange terms which are included in the second part of Eq. (16).

$$\begin{aligned}
 W_{\alpha\beta} &= -\langle \text{out}; \tilde{\alpha} | \left\{ J_{\mathbf{p}_a} (0), b_{\mathbf{p}_b}^+ (0) \right\} | \tilde{\beta}; \text{in} \rangle \\
 &+ (2\pi)^3 \sum_{n=1''2''3''b'', f''d'', \dots} \langle \text{out}; \tilde{\alpha} | J_{\mathbf{p}_a} (0) | n; \text{in} \rangle \frac{\delta^{(3)}(\mathbf{p}_b + \mathbf{P}_{\tilde{\beta}} - \mathbf{P}_n)}{E_{\mathbf{p}_b} + P_{\tilde{\beta}}^0 - P_n^0 + i\epsilon} \langle \text{in}; n | \bar{J}_{\mathbf{p}_b} (0) | \tilde{\beta}; \text{in} \rangle \\
 &- (2\pi)^3 \sum_{l=f, fb, \dots} \langle \text{out}; \tilde{\alpha} | \bar{J}_{\mathbf{p}_b} (0) | l; \text{in} \rangle \frac{\delta^{(3)}(-\mathbf{p}_b + \mathbf{P}_{\tilde{\alpha}} - \mathbf{P}_l)}{-E_{\mathbf{p}_b} + P_{\tilde{\alpha}}^0 - P_l^0} \langle \text{in}; l | J_{\mathbf{p}_a} (0) | \tilde{\beta}; \text{in} \rangle, \quad (17)
 \end{aligned}$$

where  $n = 1''2''3''b'', f''d'', \dots$  denotes the four-body states with the intermediate boson  $b''$  which denotes a photon for the three-lepton system, and  $b''$  stands for the intermediate meson for the three-barion systems. The third part of Eq. (17) describes the  $u$ -channel interaction terms which are obtained after crossing of the  $a$  and  $b$  particles. The intermediate states of this term contain one fermion  $l = f$  and one-fermion+boson  $l = f + b$  states. These diagrams are depicted in Figs. 2a and 2e.

Equation (16) contains the auxiliary amplitude

$$\mathcal{T}_{\alpha\beta} = -\langle \text{in}; \tilde{\alpha} | J_{\mathbf{p}_a} (0) | \beta; \text{in} \rangle. \quad (18)$$

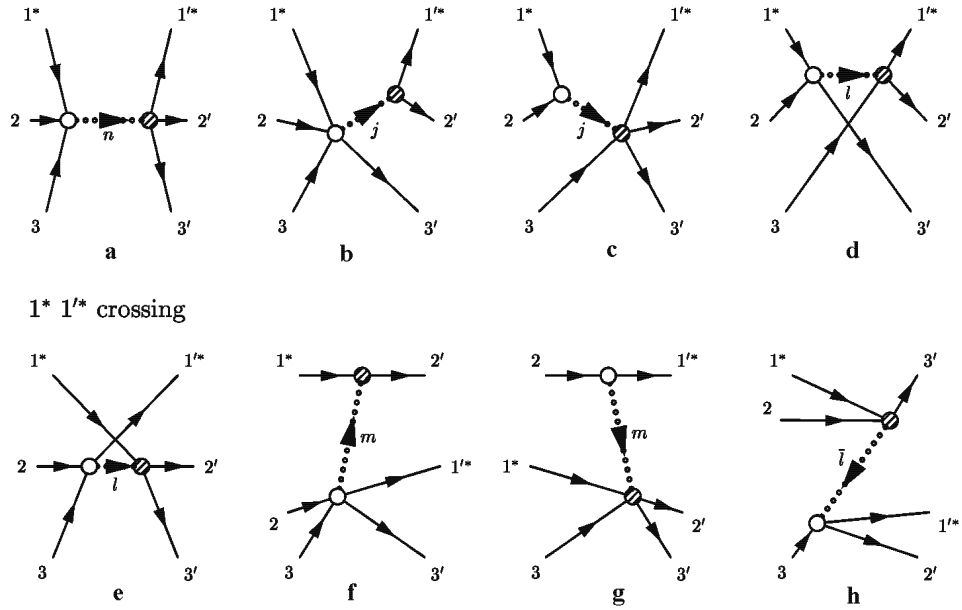


Fig. 2. The on-mass-shell particle-exchange diagrams which are included in the effective potential (20) for the three-fermion reactions  $1 + 2 + 3 \rightarrow 1' + 2' + 3'$ . The empty circle stands for the primary transition amplitude and the dashed circle corresponds to the following transition amplitude. Fermions with the index  $*$  are extracted from the asymptotic states in the expression (20) or in (17)  $a \equiv 1'$  and  $b \equiv 1$ . For any amplitude in the left side of Eq. (20) or (17), only one particle ( $a$  or  $b$ ) is considered off mass shell. All of diagrams have the three-dimensional time-ordered form with the “dressed” vertices. Therefore, in all of the diagrams the initial hollow circle is depicted on left-hand side and the following circle takes place in the right-hand side.

In the transition matrix  $\langle \tilde{\alpha} | J_{\mathbf{p}_a}(0) | \beta \rangle$  with arbitrary  $\tilde{\alpha}$  and  $\beta$  states, all particles except  $a$  are on the mass shell. The four-momentum of particle  $a$  is expressed through the four-momenta of other on mass shell particles, i.e.  $p_a = P_\beta - P_{\tilde{\alpha}}$ . Therefore, we shall later consider particle  $a$  as an off-mass-shell particle in the corresponding matrix element.

For the one-particle asymptotic state  $\tilde{\alpha} \equiv 1'$  we have  $f_{1'+a,\beta} = \mathcal{T}_{1'+a,\beta}$ , because  $\langle \text{out}; 1' | = \langle \text{in}; 1' |$ . For the three-particle asymptotic state  $\langle \text{out}; \alpha |$ , the situation is more complicated,  $\mathcal{T}_{1'+2'+a,\beta} \neq \mathcal{T}_{1'+2'+a,\beta}$ . We can obtain the analogue to (16) for  $\mathcal{T}_{\alpha\beta}$  (18) using the  $S$ -matrix reduction formulae

$$\mathcal{T}_{\alpha\beta} = w_{\alpha\beta} + (2\pi)^3 \sum_{\gamma} \mathcal{T}_{\alpha\gamma} \frac{\delta^{(3)}(\mathbf{p}_b + \mathbf{P}_{\tilde{\beta}} - \mathbf{P}_{\gamma})}{E_{\mathbf{p}_b} + P_{\tilde{\beta}}^0 - P_{\gamma}^0 + i\epsilon} \mathcal{T}_{\beta\gamma}^*, \quad (19)$$

where

$$\begin{aligned}
 w_{\alpha\beta} = & -\langle \text{in}; \tilde{\alpha} | \left\{ J_{\mathbf{p}_a}(0), b_{\mathbf{p}_b}^+(0) \right\} | \tilde{\beta}; \text{in} \rangle \\
 & + (2\pi)^3 \sum_{n=1''2''3''b'', \dots} \langle \text{in}; \tilde{\alpha} | J_{\mathbf{p}_a}(0) | n; \text{in} \rangle \frac{\delta^{(3)}(\mathbf{p}_b + \mathbf{P}_{\tilde{\beta}} - \mathbf{P}_n)}{E_{\mathbf{p}_b} + P_{\tilde{\beta}}^0 - P_n^0 + i\epsilon} \langle \text{in}; n | \bar{J}_{\mathbf{p}_b}(0) | \tilde{\beta}; \text{in} \rangle \\
 & - (2\pi)^3 \sum_{l=f, fb, \dots} \langle \text{in}; \tilde{\alpha} | \bar{J}_{\mathbf{p}_b}(0) | l; \text{in} \rangle \frac{\delta^{(3)}(-\mathbf{p}_b + \mathbf{P}_{\tilde{\alpha}} - \mathbf{P}_l)}{-E_{\mathbf{p}_b} + P_{\tilde{\alpha}}^0 - P_l^0} \langle \text{in}; l | J_{\mathbf{p}_a}(0) | \tilde{\beta}; \text{in} \rangle. \quad (20)
 \end{aligned}$$

Using Eqs. (16) and (18), we can find the connection formula between  $f_{\alpha\beta}$  and  $\mathcal{T}_{\alpha\beta}$ . If we suppose, that

$$\mathcal{T}_{\alpha\beta} = \left( w W^{-1} f \right)_{\alpha\beta} \quad (21a)$$

and

$$f_{\alpha\beta} = \left( W w^{-1} \mathcal{T} \right)_{\alpha\beta}, \quad (21b)$$

then after insertion of relation (21a) into Eq. (16), we obtain Eq. (18) for  $\mathcal{T}_{\alpha\beta}$ . And vice versa, after insertion of relation (21b) into Eq. (18), we get Eq. (16). This is the justification of the relations (21) for the nonsingular effective three-body potentials  $W$  (17) and  $w$  (20).

The consistent procedure of separation of the complete set of a connected and disconnected parts in the three-dimensional equations (19) or (16) is well known as field-theoretical cluster decomposition procedure [9,10]. In Ref. [8], this procedure is applied to the three-body equation for the  $\gamma\pi N$  systems. For the three-body reactions  $1 + 2 + 3 \rightarrow 1' + 2' + 3'$ , the cluster decomposition procedure is the same as separation of the following connected and disconnected matrix elements

$$\begin{aligned}
 \mathcal{T}_{1'2'3',123}^{dc} = & -\langle \text{in}; \mathbf{p}'_2, \mathbf{p}'_3 | b_{\mathbf{p}'_3}^+(\text{in}) J_{\mathbf{p}'_1}(0) | \mathbf{p}_1, \mathbf{p}_2; \text{in} \rangle \\
 & + \langle \text{in}; \mathbf{p}'_2, \mathbf{p}'_3 | b_{\mathbf{p}'_2}^+(\text{in}) J_{\mathbf{p}'_1}(0) | \mathbf{p}_1, \mathbf{p}_3; \text{in} \rangle - \langle \text{in}; \mathbf{p}'_2, \mathbf{p}'_3 | b_{\mathbf{p}'_1}^+(\text{in}) J_{\mathbf{p}'_1}(0) | \mathbf{p}_2, \mathbf{p}_3; \text{in} \rangle \\
 & + \langle \text{in}; \mathbf{p}'_2 | J_{\mathbf{p}'_1}(0) b_{\mathbf{p}'_3}(in) | \mathbf{p}_1, \mathbf{p}_2, \mathbf{p}_3; \text{in} \rangle - \langle \text{in}; \mathbf{p}'_3 | J_{\mathbf{p}'_1}(0) b_{\mathbf{p}'_2}(in) | \mathbf{p}_1, \mathbf{p}_2, \mathbf{p}_3; \text{in} \rangle, \\
 \mathcal{T}_{1'2'3',123}^c = & - \sum_{\text{permutations } 1,2,3} \langle \text{in}; \mathbf{p}'_2, \mathbf{p}'_3 | \left\{ \left\{ J_{\mathbf{p}'_1}(0), b_{\mathbf{p}'_1}^+(\text{in}) \right\}, b_{\mathbf{p}'_2}^+(\text{in}) \right\} | \mathbf{p}_3; \text{in} \rangle. \quad (23)
 \end{aligned}$$

The  $s$  and  $u$  channel terms of the effective potential (20) are depicted in Figs. 2a and 2e. As off-mass-shell one-particle states are taken  $b = 1$  and  $a = 1'$ . These off-mass-shell particles in the following figure are marked by \*. The diagrams in Figs. 2a and 2e have different chronological sequences of the absorption and the emission of particles 1 and 1'. In particular, the  $s$ -channel diagram 2a corresponds to the chain of reactions, where firstly the initial three-body state  $1^* + 2 + 3$  transforms

into intermediate on-mass-shell  $n$ -particle states which afterwards produce the final  $1^{*'} + 2' + 3'$  state. In the diagram 2e, at first the final fermion  $1^{*'}$  is generated with the intermediate states  $l$  from the initial  $2 + 3$  states, and afterwards we obtain final  $2' + 3'$  state from the intermediate  $l + 1^*$  states.

Using the cluster decomposition procedure for the  $s$  and  $u$  channel terms in Eq. (20) or in Eq. (25), one can change the chronological sequence of absorption of the initial on-mass-shell fermions  $2, 3$  and emission of the final on-mass-shell particles  $2', 3'$ . The diagrams 2b, 2c and 2d show all possible transpositions of the particles  $3$  and  $3'$  from the original  $s$ -channel diagram 2a which can be performed after transposition of particles  $3$  and  $3'$  using the disconnected structure (22) of the tree-body amplitudes. In particular, Fig. 2b is obtained after transposition of fermion  $3'$  i.e. after substitution of the disconnected part of amplitude  $\langle \text{in}; \mathbf{p}'_2 | J_{\mathbf{p}'_1}(0) b_{\mathbf{p}'_3}(\text{in}) | n; \text{in} \rangle$ . Fig. 2c is generated by transposition of fermion  $3$  and Fig. 2d is the result of the permutation of both particles  $3$  and  $3'$ . Unlike to the diagram 2a, in the diagram 2b the intermediate  $l$  states arise together with the final  $3'$  state and subsequently are generating the final two-fermion  $1^{*'} + 2'$  states. The same procedure of transposition of particles  $3$  and  $3'$  from the  $u$ -channel diagram in Fig. 2e generates the diagrams 2f, 2g and 2h. Another kind of permutations of both particles  $2 + 3$  and  $2' + 3'$  from  $s$ -channel diagram in Fig. 2a produces the diagrams 3a, 3b and 3c. In particular, diagrams 3g and 3i are obtained from diagrams 2b and 2f after transposition of the  $2 + 3$  particle states. And transposition of  $2' + 3'$  states in diagrams 2c and 2g produces diagrams 3h and 3j. The complete set of the diagrams which can be obtained after transpositions of the particles  $(2, 3); (2'3')$  consists of the different disposition of these particles at the first vertex function and at the following vertex function. The first vertex function in Fig. 2 and in Fig. 3 is denoted with the hollow circle in Fig. 2 and the dashed circle stands for the next vertex function. One has the following combinations of the dispositions of particles  $(2, 3); (2'3')$  at the vertex functions:

$$\begin{aligned} 1^* + \text{zero particles} &\implies 1^{*'} + \text{four particles}, \\ 1^* + \text{one particle} &\implies 1^{*'} + \text{three particles}, \\ 1^* + \text{two particles} &\implies 1^{*'} + \text{two particles}, \\ 1^* + \text{three particles} &\implies 1^{*'} + \text{one particle and} \\ 1^* + \text{four particles} &\implies 1^{*'} + \text{zero particles}. \end{aligned}$$

For instance, we have four diagrams

$$\begin{aligned} 1^* + 2 &\implies 1^{*'} + 3, 2'3' \text{ (Fig. 2c)}, \\ 1^* + 3 &\implies 1^{*'} + 2, 2'3', \\ 1^* + 2' &\implies 1^{*'} + 23, 3' \text{ and} \\ 1^* + 3' &\implies 1^{*'} + 23, 2' \text{ (Fig. 3g)} \end{aligned}$$

for the disposition

$$1^* + \text{one particle} \implies 1^{*'} + \text{three particles}.$$

The particle distribution

$$1^* + \text{three particles} \implies 1^{*'} + \text{one particle}$$

has also four diagrams

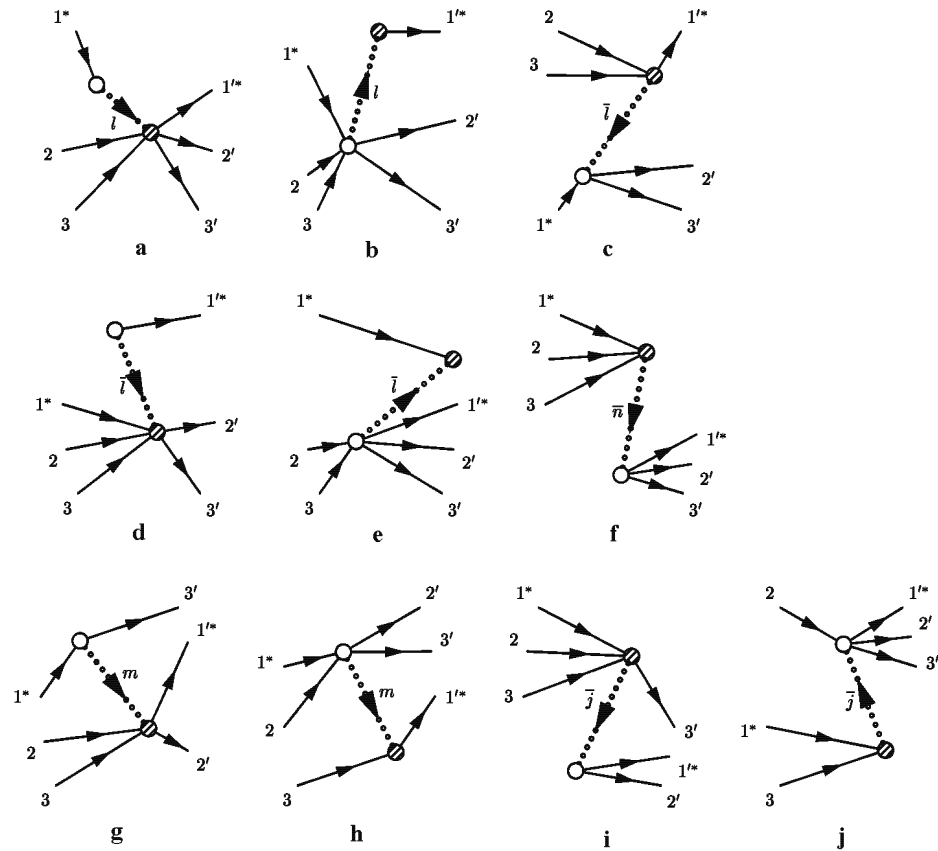


Fig. 3. Diagrams obtained after the two particle (2,3) and (2',3') transposition from the s-channel diagram in Fig. 2a and from the t-channel diagram in Fig. 2e.

$$\begin{aligned}
 1^* + 3, 2'3' &\Rightarrow 1'^* + 2, \\
 1^* + 2, 2'3' &\Rightarrow 1'^* + 3 \text{ (Fig. 3h),} \\
 1^* + 23, 3' &\Rightarrow 1'^* + 2' \text{ (Fig. 2b),} \\
 1^* + 23, 2' &\Rightarrow 1'^* + 3'.
 \end{aligned}$$

The particle distribution

$$1^* + \text{two particles} \Rightarrow 1'^* + \text{two particles}$$

can be observed in the six diagrams

$$\begin{aligned}
 1^* + 23 &\Rightarrow 1'^* + 2'3' \text{ (Fig. 2a),} \\
 1^* + 2, 3' &\Rightarrow 1'^* + 3, 2' \text{ (Fig. 2d),} \\
 1^* + 2, 2' &\Rightarrow 1'^* + 3, 3', \\
 1^* + 3, 2' &\Rightarrow 1'^* + 2, 3', \\
 1^* + 3, 3' &\Rightarrow 1'^* + 2, 2' \text{ and} \\
 1^* + 2'3' &\Rightarrow 1'^* + 23 \text{ (Fig. 3c).}
 \end{aligned}$$

The diagrams

$$1^* \implies 1'^* + 23, 2'3' \text{ (Fig. 3a) and}$$

$$1^* + 23, 2'3' \implies 1'^* \text{ (Fig. 3b)}$$

are related to the distributions

$$1^* + \text{zero particles} \implies 1'^* + \text{four particles} \text{ and } 1^* +$$

$$\text{four particles} \implies 1'^* + \text{zero particles},$$

correspondingly.

Thus the  $s$ -channel term in Eq. (25) generates the  $2 \times 4 + 6 + 2 = 16$  connected terms after cluster decomposition. The other 16 connected terms produce the  $u$ -channel term in Eq. (25). Hence, we get 32 independent skeleton diagrams after the cluster decomposition procedure performed in the second and in the third terms of Eq. (20) or Eq. (25). Diagrams 3c, 3d, 3e, 3f, 3i and 3j contain the antiparticle intermediate states, because the time-ordered field-theoretical formulation includes the complete set of the intermediate particle propagators with different time sequences. This means that for any diagrams with  $n, l, \dots$ -particle intermediate states, there appear the corresponding diagrams with the antiparticle  $\bar{n}, \bar{l}, \dots$  intermediate states.

The  $S$ -matrix reduction formulas for the  $1d \implies 1' + d'$  process gives the following equation

$$\mathcal{T}_{1'd',1d} = -\langle \text{out}; \mathbf{P}'_d | J_{\mathbf{P}'_1}(0) | \mathbf{P}_1, \mathbf{P}_d; \text{in} \rangle = w_{1'd',1d}$$

$$+ (2\pi)^3 \sum_{n=3f,fd,d3} \mathcal{T}_{1'd',\gamma} \frac{\delta^{(3)}(\mathbf{p}_1 + \mathbf{P}_d - \mathbf{P}_\gamma)}{E_{\mathbf{p}_1} + P_d^o - P_\gamma^o + i\epsilon} \mathcal{T}_{1d,\gamma}^*, \quad (24)$$

where

$$w_{1'd',1d} = -\langle \text{out}; \mathbf{P}'_d | \left\{ J_{\mathbf{P}'_1}(0), b_{\mathbf{p}_1}^\dagger(0) \right\} | \mathbf{P}_d; \text{in} \rangle \quad (25)$$

$$+ (2\pi)^3 \sum_{n=1'2'3'b'',\dots} \langle \text{out}; \mathbf{P}'_d | J_{\mathbf{P}'_1}(0) | n; \text{in} \rangle \frac{\delta^{(3)}(\mathbf{p}_1 + \mathbf{P}_d - \mathbf{P}_n)}{E_{\mathbf{p}_1} + P_d^o - P_n^o + i\epsilon} \langle \text{in}; n | \bar{J}_{\mathbf{P}_d}(0) | \mathbf{P}_d; \text{in} \rangle$$

$$- (2\pi)^3 \sum_{l=f,fb,\dots} \langle \text{out}; \mathbf{P}'_d | \bar{J}_{\mathbf{P}'_1}(0) | l; \text{in} \rangle \frac{\delta^{(3)}(-\mathbf{p}_b + \mathbf{P}_\alpha - \mathbf{P}_l)}{-E_{\mathbf{p}_1} + P_d^o - P_l^o} \langle \text{in}; l | J_{\mathbf{P}'_1}(0) | \mathbf{P}_d; \text{in} \rangle.$$

Equations (24) and (25) for the amplitude and for the effective potential of the  $1d$  scattering reaction have the same form as the two-body equations. After cluster decomposition of  $w_{1'd',1d}$ , we obtain only 6 terms (see Fig. 4) with a transposition  $d \iff d'$  and with crossing transformation  $1' \iff 1$ . Equation (24) contains the  $1d \rightarrow 1'2'3'$  transition matrix which is connected with the  $123 \rightarrow 1'2'3'$  transition amplitude according to Eq. (19), where  $\alpha, \beta = 3f$ , but  $\gamma = 3f, fd$ . Thus the  $123 \rightarrow 1'2'3'$ ,  $1d \rightarrow 1'2'3'$  and  $1d \rightarrow 1'd'$  transition amplitudes are the solutions of the coupled equations (19) and (24). Using the linearization procedure of such type equations [8,11], one can obtain the equivalent set of Lippmann-Schwinger-type equations

$$\mathcal{T}_{\alpha,fd}(E_{fd}) = U_{\alpha,fd}(E_{fd}) + \sum_{\gamma} U_{\alpha\gamma}(E_{fd}) \frac{1}{E_{fd} - E_\gamma + i\epsilon} \mathcal{T}_{\gamma,fd}(E_{fd}), \quad (26)$$

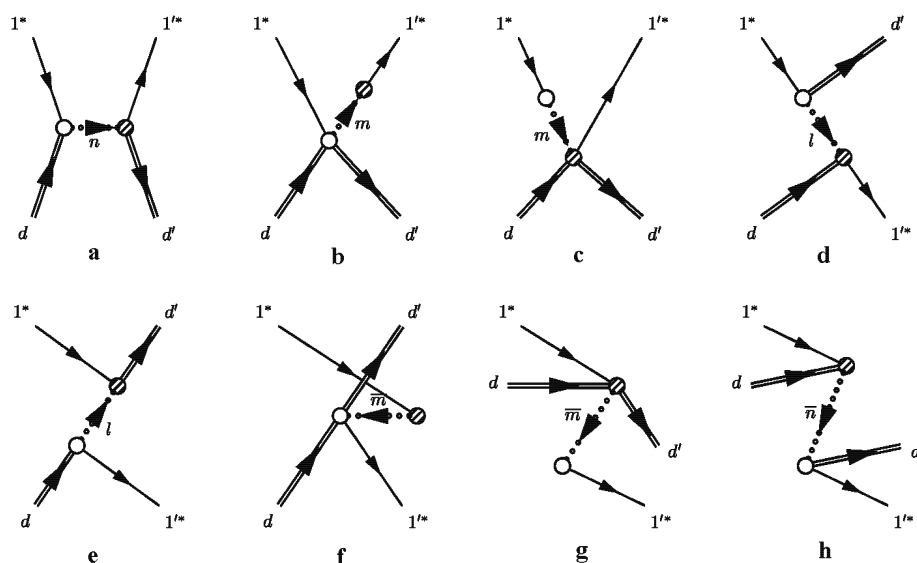


Fig. 4. Graphical representation of the on-mass-shell particle-exchange potential (25) for the  $1 + d \Rightarrow 1' + d'$  amplitude after cluster decomposition. The double line denotes a two-fermion bound state,  $n$  stands for the three-fermion+boson states,  $m = f + b, \dots$  and  $l$  corresponds to the intermediate fermion  $f, f + b, \dots$  states.

where  $E_{fd} = E_d + E_f$  is the energy of the asymptotic fermion and two-fermion bound state  $d$ ,  $\alpha, \gamma = 3f, fd$ , and  $U_{\alpha\gamma}(E)$  is unambiguously determined from the connected part of potentials  $w_{\alpha\gamma}$  according to the relation (9a). Note that the solution of the three-body equations (i.e. the  $123 \rightarrow 1''2''3'$  and  $123 \rightarrow 3'd''$  transition amplitudes) participates in the  $w_{\alpha\gamma}^c$  potential in the diagrams 3b and 3c. One can get rid of the three-fermion potential of such type nonlinearities after introduction of new amplitudes  $f_{\alpha,\beta} = F_{\alpha,\beta} + A_{\alpha,\beta}$  in Eq. (19) and in Eq. (24), where the choice of  $A_{\alpha,\beta}$  is conditioned by the cancellation of the terms in Figs. 2b and 2c which have the form  $fg_oA^+$  and  $Ag_o f^+$ . Then we get the linear Lippmann-Schwinger-type equation for  $F_{\alpha,\beta}$  amplitudes with the disconnected terms. Therefore this linearization procedure generates necessity to use the Faddeev-type equations for the three-fermion scattering problems. Certainly, in the intermediate energy region, i.e. up to 2 GeV of the energy of the incoming proton for the Nd-3N systems, one can neglect the diagrams 3i and 3j with the  $2\bar{N}$  states and the diagram 3f with the  $3\bar{N}$  intermediate state.

Equations (19) and (24) represent the spectral decomposition formulae (or off-shell unitarity conditions) for the three-body amplitudes in the standard quantum field theory. Such three-dimensional time-ordered relations were considered in the textbooks in the quantum field theory [5,6,9] and in the nonrelativistic collision theory [3,4] for the two-body reactions. Therefore, one can treat Eqs. (19) and (24) as the three-body generalization of the field-theoretical spectral decomposition

formulae (or off-shell unitarity conditions) for the two-body amplitudes. The field-theoretical formulation allows us to obtain the analytical structure of the three-body amplitudes, and the problem of determination of the three-body forces in the nonrelativistic Faddeev equations does not arise in the considered formulation.

#### 4. Equal-time anticommutators as an off-mass-shell particle-exchange potential

The important part of the effective potential  $w_{\alpha\beta}$  is the equal-time commutator in the effective potentials (20) and (25). The equal-time anticommutators in the effective potential of the  $1d \rightarrow 1'd'$ ,  $1d \rightarrow 1'2'3'$  and  $123 \rightarrow 1'2'3'$  reactions are

$$Y_{1d,1'd'} = - \langle \mathbf{P}'_d | \{ J_{\mathbf{P}'_1}(0), b_{\mathbf{P}_1}^+(0) \} | \mathbf{P}_d; \text{in} \rangle, \quad (27a)$$

$$Y_{1d,1'2'3'} = - \langle \mathbf{P}'_2, \mathbf{P}'_3 | \{ J_{\mathbf{P}'_1}(0), b_{\mathbf{P}_1}^+(0) \} | \mathbf{P}_d; \text{in} \rangle, \quad (27b)$$

$$Y_{123,1'2'3'} = - \langle \mathbf{P}'_2, \mathbf{P}'_3 | \{ J_{\mathbf{P}'_1}(0), b_{\mathbf{P}_1}^+(0) \} | \mathbf{P}_2, \mathbf{P}_3; \text{in} \rangle. \quad (27c)$$

The explicit form of expressions (27) can be determined using the *a priori* given Lagrangian and equal-time anticommutations relation between the Heisenberg field operators. In the case of renormalizable Lagrangian models or for nonrenormalizable simple phenomenological Lagrangians, the equal-time anticommutators are easily calculated [8,11]. In that case, expressions (27), which are often called the seagull terms, consist of the off-shell-**internal** one-particle-exchange potentials (see diagrams 5a, 5c and 5e), and of the contact (overlapping) terms (Figs. 5b, 5d and 5f) which do not contain any particle propagator in the intermediate states between asymptotic  $|\bar{\beta}\rangle$  and  $\langle\bar{\alpha}|$  states. The equal-time commutators are the only part of effective potentials (20) or (25) which contains **explicitly** the **internal** off-mass-shell particle-exchange diagrams, since other terms in the effective potential (20) or (25) consist of the on-mass-shell particle-exchange terms, where off-mass-shell are **external** fermions. In order to clarify the structure of the equal-time terms, we will consider Lagrangian of the simplest  $\phi^3$  model for the electromagnetic fields and for the pseudoscalar  $\pi N$  interactions

$$\mathcal{L}_{em} = -e\bar{\psi}\gamma^\mu\psi A_\mu; \quad \mathcal{L}_{ps} = -ig_\pi\bar{\Psi}\gamma_5\tau\Phi_\pi\Psi. \quad (28)$$

The current operator and the equation of motion for these Lagrangians are

$$\partial_\nu\partial^\nu A_\mu = J_\mu = -e\bar{\psi}\gamma^\mu\psi \quad \text{and} \quad (\partial_\nu\partial^\nu + m_\pi^2)\Phi_\pi^i = j_\pi^i = -ig_\pi\bar{\Psi}\gamma_5\tau^i\Psi \quad (29)$$

Using the equal-time anticommutation relation between the Heisenberg field operators for the expressions (27), we get

$$\begin{aligned} Y_{\alpha\beta} &= \frac{-e}{\sqrt{Z_1 Z_{1'}}} \bar{u}(\mathbf{P}'_1)\gamma^\mu u(\mathbf{P}_1) \langle \text{in}; \tilde{\alpha} | A_\mu(0) | \tilde{\beta}; \text{in} \rangle \\ &= \frac{-e}{\sqrt{Z_1 Z_{1'}}} \frac{\bar{u}(\mathbf{P}'_1)\gamma^\mu u(\mathbf{P}_1)}{(P_\alpha^- - P_\beta^-)^2} \langle \text{in}; \tilde{\alpha} | J_\mu(0) | \tilde{\beta}; \text{in} \rangle, \end{aligned} \quad (30a)$$

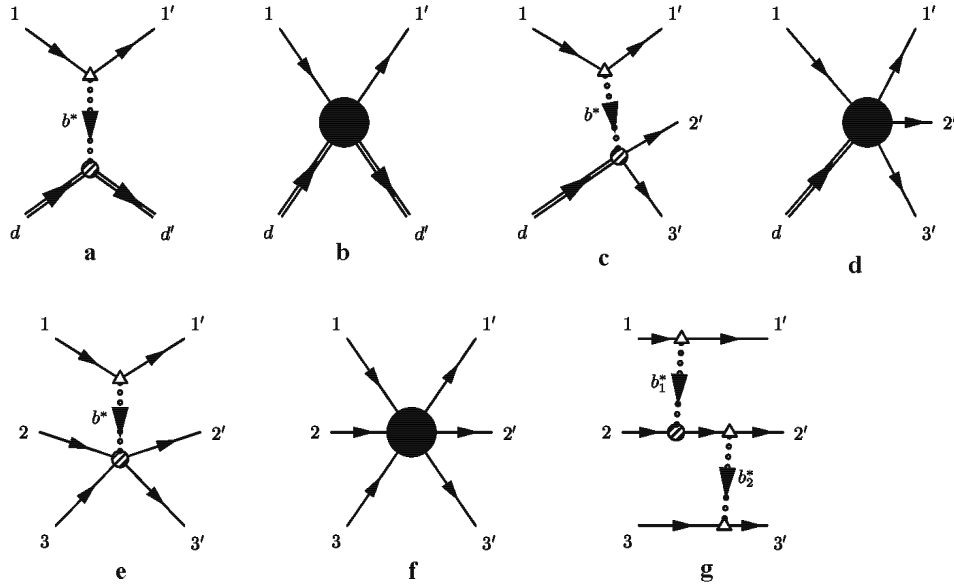


Fig. 5. Graphical representation of the equal-time anticommutators (27). These terms are shown separately for the binary reactions (a and b), for the process  $2 \Rightarrow 3'$  (c and d) and for the three-body process  $3 \Leftrightarrow 3'$  (e, f and g). Diagrams a, c and e correspond to one of the off-mass-shell particle-exchange interactions which are appearing from in the  $\phi^3$ -theory, i.e., for the QED or for the Yukawa-type interactions. The triangle denotes the vertex functions in the tree approximation. Diagrams b, d and f describe the contact (overlapping) interaction which does not contain the intermediate hadron propagation between hadron states. Diagram 5g corresponds to the simplest one off-mass-shell boson fermion and two off-mass-shell boson-exchange interaction which is obtained from the equal-time commutators in Eq. (27c) (diagram 5F) in the framework of the  $\phi^3$  theory.

or for the  $\pi$ NN system

$$\begin{aligned}
 Y_{\alpha\beta} &= \frac{-ig_\pi}{\sqrt{Z_1 Z_{1'}}} \bar{u}(\mathbf{p}_1') \gamma^5 \tau^i u(\mathbf{p}_1) \langle \text{in}; \tilde{\alpha} | \phi_\pi^i(0) | \tilde{\beta}; \text{in} \rangle \\
 &= \frac{-ig_\pi}{\sqrt{Z_1 Z_{1'}}} \frac{\bar{u}(\mathbf{p}_1') \gamma^5 \tau^i u(\mathbf{p}_1)}{(P_\alpha - P_\beta)^2 - m_\pi^2} \langle \text{in}; \tilde{\alpha} | j_\pi^i(0) | \tilde{\beta}; \text{in} \rangle, \quad (30b)
 \end{aligned}$$

where  $\tilde{\alpha}, \tilde{\beta} = (d, d'), (d, 2'3'), (23, 2'3')$  for (27a), (27b) and (27c), correspondingly. Expressions (27a) or (27b) relate to the one off-mass-shell boson exchange diagrams 5a, 5c and 5e for the Lagrangians (28). Using more complete Lagrangian models, one can obtain also heavy  $\rho, \omega$  meson exchange diagrams [8,11]. Moreover, in Ref. [11] the one-boson-exchange (OBE) Bonn model of the NN potential was exactly reproduced from the equal-time anticommutators. There were also numeri-

cally estimated the contributions from the contact (overlapping) terms for NN phase shifts. These contact (overlapping) terms arise from the  $\phi^4$  (four-point) part of Lagrangians or from the nonrenormalizable Lagrangians, and they play an important role for the NN scattering.

The other source of the overlapping (contact) terms in the quantum field theory are the quark-gluon degrees of freedom. One can construct the hadron creation and annihilation operators, as well as the Heisenberg field operators of hadrons, from the quark-gluon fields within the framework of the Haag–Nishijima–Zimmermann [14] treatment of composite particles. In that case, the contact terms (see diagrams 5b, 5d and 5f) contain the contributions from the quark-gluon exchange [11,12]. However, equations (19), (20), (24) and (25) remain the same also for the formulation with the quark-gluon degrees of freedom.

The contact (overlapping) terms shown in diagrams 5c, 5d and 5e, 5f can be treated as pure three-body forces. For these terms, it is necessary to use an additional derivation of two-body and the three-body equations like the spectral decomposition formulae (19). These extra auxiliary two-body and the three-body amplitudes are necessary for the solution of the considered three-body equations. As an example, we shall consider the amplitude  $\langle \mathbf{p}'_2, \mathbf{p}'_3 | j_b(0) | \mathbf{p}_2, \mathbf{p}_3 \rangle$  for the reaction  $23 \rightarrow b'2'3'$ . This amplitude participates in the diagram 5e, and the corresponding on-mass-shell particle-exchange diagrams are depicted in Fig. 6. Diagrams 6b, 6c, 6d are obtained from the  $s$ -channel diagram 6a after transpositions  $2 \leftrightarrow 1'$ . The next four diagrams are produced by the crossing permutation of the off-mass-shell particles  $1^*$  and  $b'^*$ . The last four diagrams are obtained from diagrams 6a, 6c, 6e and 6c after transposition of the  $1'2'$  states to the first vertex.

The complete set of the diagrams which can be obtained after transpositions of the particles  $2; 1'2'$  in the  $s$  channel term of amplitude of the  $1^* + 2 \Rightarrow b'^*1'2'$  reactions consists from the following dispositions of on mass shell particles  $2; (1'2')$  at the first and the next vertices:

- $1^* + \text{zero particles} \Rightarrow b'^* + \text{three particles},$
- $1^* + \text{one particle} \Rightarrow b'^* + \text{two particles},$
- $1^* + \text{two particle} \Rightarrow b'^* + \text{two particles and}$
- $1^* + \text{three particles} \Rightarrow b'^* + \text{zero particles}.$

For instance, we have three diagrams

- $1^* + 2 \Rightarrow b'^* + 1'2'$  (Fig. 6a),
- $1^* + 1' \Rightarrow b'^* + 2, 2'$ (Fig. 6d) and
- $1^* + 2' \Rightarrow b'^* + 2, 2'$

for the distribution

$$1^* + \text{one particle} \Rightarrow b'^* + \text{two particles}.$$

The particle dispositions

$$1^* + \text{two particles} \Rightarrow b'^* + \text{one particle}$$

can be realized also with the three diagrams

- $1^* + 2, 1' \Rightarrow b'^* + 2',$
- $1^* + 2, 2' \Rightarrow b'^* + 1'$  (Fig. 6b) and
- $1^* + 1'2' \Rightarrow b'^* + 2$  (Fig. 6j).

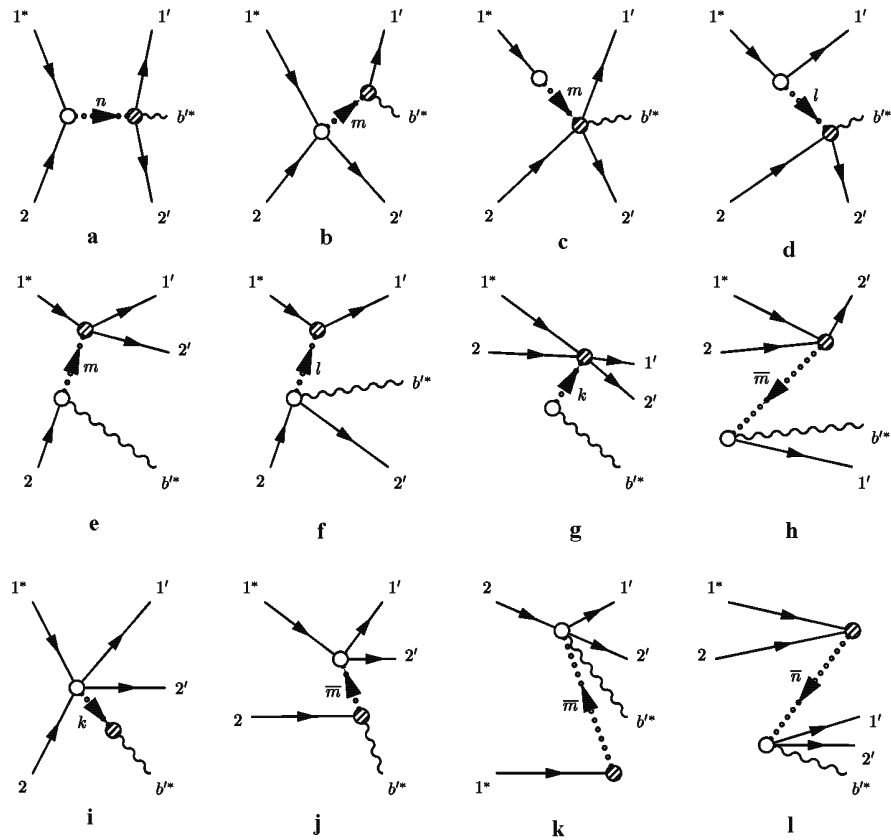


Fig. 6. Graphical representation of the on-mass-shell particle-exchange potential for the  $1 + 2 \Rightarrow 1' + 2' + b'$  amplitude with off-mass-shell boson  $b'$ . This amplitude arises in the seagull term (4.1c) in the  $\phi^3$  theory after cluster decomposition. The curled line denotes the off-mass-shell boson  $b'^*$  which corresponds to the photon  $\gamma$  for leptons or  $\pi$ -meson for barions.  $n = 2f'' + b'', 2f'' + 2b'', d'' + b'', \dots$  stands for the intermediate on-mass-shell particle states in  $s$  channel,  $m = f'' + b'', \dots$  and  $l = b'', 2b'', \dots$

And the diagrams with the particle distribution

$$1^* + 2, 1'2' \Rightarrow b'^* \text{ (Fig. 6i) and}$$

$$1^* \Rightarrow b'^* + 2, 1'2' \text{ (Fig. 6c)}$$

form the distributions

$$1^* + \text{three particles} \Rightarrow b'^* + \text{zero particles and}$$

$$1^* + \text{zero particles} \Rightarrow b'^* + \text{three particles.}$$

Therefore, the complete set of the connected  $s$ -channel terms counts  $2 \times 3 + 2 = 8$  terms. Together with the  $u$  channel terms, we have 32 diagrams for the  $b$ -boson creation reaction on the two fermion system.

The simplest contact terms (27c) for the three-point Lagrangians (28) have the form

$$\begin{aligned}
 Y_{1'2'3',123} &= -e^3 \frac{\bar{u}(\mathbf{p}'_1)\gamma^\mu u(\mathbf{p}_1)}{(P_{2'+3'} - P_{2+3})^2} \langle \mathbf{p}'_2 | J_\nu(0) | \mathbf{p}_2 \rangle \\
 &\times \frac{\bar{u}(\mathbf{p}'_3)\gamma^\nu (\gamma^\sigma Q_\sigma + m_{el})\gamma_\mu u(\mathbf{p}_3)}{Z_1 Z_3 (p'_3 - p_3)^2 (Q^2 - m_{el}^2)} \quad (31a)
 \end{aligned}$$

and for the  $\pi$ NN system

$$\begin{aligned}
 Y_{1'2'3',123} &= -i^3 g_\pi^3 \frac{\bar{u}(\mathbf{p}'_1)\gamma^5 \tau^i u(\mathbf{p}_1)}{(P_{2'+3'} - P_{2+3})^2 - m_\pi^2} \langle \mathbf{p}'_2 | j_\pi^k(0) | \mathbf{p}_2 \rangle \\
 &\times \frac{\bar{u}(\mathbf{p}'_3)\gamma^5 \tau^k (\gamma^\sigma Q_\sigma + m_N)\gamma_5 \tau^i u(\mathbf{p}_3)}{Z_1 Z_3 \left( (p'_3 - p_3)^2 - m_\pi^2 \right) (Q^2 - M_N^2)}, \quad (31b)
 \end{aligned}$$

where  $Q = p_1 + p_2 - p'_1$ , and this simplest two-off-mass-shell boson-exchange term is depicted in Fig. 5g.

Starting from any Lagrangian, we always obtain one-off-mass-shell boson-exchange potentials (Figs. 5a, 5c and 5e). For the contact (overlapping) terms we use  $\phi^4$  terms in Lagrangian [8], or more complicated models of phenomenological Lagrangians [11], models of a nonrenormalizable Lagrangian, quark-gluon degrees of freedom [8] etc. These terms contains another kind of a three-body amplitudes, too, and one must include these extra-auxiliary two-body and three-body amplitudes in the set of coupled equations (19) and (24). Thus the number of the solved three-body equations and the form of the auxiliary amplitudes is depending on the form of "input" Lagrangian. This means that the unified description of the coupled three-fermion reactions can help us to determine the form of input Lagrangians which are sufficient and necessary for a description of the experimental observables.

Besides the Lagrangians, as "input" by construction of the effective three-body potentials are the amplitudes of the  $2 \rightarrow 2'$  and  $2 \rightarrow 3'$  reactions and the three-point vertex functions. In these vertex functions, two particles are on mass shell and they are function of one variable. Therefore, one can determine these vertex functions from experimental data using the quark counting rules, dispersion relations, the Regge trajectories theory, or the inverse scattering method [13].

## 5. Summary

In this paper, I have considered the three-dimensional covariant scattering equations for the amplitudes of the three-fermion scattering reactions. The basis for these three-body relativistic equations are the standard field-theoretical  $S$ -matrix reduction formulae. After decomposition over the complete set of the asymptotic

“in” states, the quadratically nonlinear three-dimensional equations (19) or (24) are derived. These equations have the same form as the off-shell unitarity conditions (1) in the nonrelativistic collision theory. The suggested nonlinear equations can be replaced by the equivalent Lippmann–Schwinger type equations (2) or (16) for the connected parts of the three-body amplitudes. If one want to get rid of the potential of these three-body equations from the nonlinear terms (see diagrams in Figs. 2b and 2c with  $j = f''f''$ ), after some simple transformations, one obtains the Lippmann–Schwinger-type equations with the usual disconnected terms (see the last three diagrams in Fig. 1c) of a three-body potential. In this case, instead of Eq. (16) we get the Faddeev-type equations. Equations (16) satisfy all first principles of the quantum field theory. Moreover, as “INPUT” for construction of the potential of these equations are required the one-variable vertex functions which can be determined from the dispersion relations, or from the inverse scattering method, i.e., they can be obtained from the two-body scattering observables.

The effective potential of the suggested equations consists (i) of the on mass shell particle exchange diagrams in Figs. 2–4 and (ii) of the equal-time commutators which contain one of the off-mass-shell boson-exchange diagrams (Figs. 5a, 5c and 5d) and overlapping (contact) terms (Figs. 5b, 5d and 5e). The form and the number of these equal-time potentials depend on the input Lagrangian model. For the three-lepton interactions, the overlapping (contact) terms do not appear and the diagram in Fig. 5e is reduced to the simple off mass shell two-photon exchange diagram in Fig. 5f. In the case of the two-body reactions, the equal-time commutators generate effective potential which can be constructed from the phenomenological one-variable vertex functions if one uses the simple phenomenological Lagrangians. These one-variable vertex functions could also be determined from experimental observables.

In order to construct the three-fermion potential from the one-variable phenomenological vertices, one needs also to construct the two-fermion scattering amplitudes, the two-fermion  $\Rightarrow$  two-fermion + boson transition amplitudes (see Figs. 5e and 6) and also the complicated overlapping (contact) term (Figs. 5d and 5f). The main attractive feature of the considered field-theoretical scheme of the three-body equation is that it allows to estimate the importance of the overlapping (contact) terms. Therefore, the unified description of two-body and three-body reactions in the considered formulation allows to determine the form of the simplest Lagrangians which are necessary and sufficient for the unified description of the two-body and the three-body experimental data. In addition, these calculations allows an improvement of the accuracy of the calculations in the tree and in the Born approximations.

The considered field-theoretical formulation is not less general than the four-dimensional Bethe–Salpeter equations. The final form of the equations (20) or (24) do not depend on the choice of the Lagrangian and these equations are valid for any QCD-motivated model with the quark-gluon degrees of freedom. But the suggested equations are much simpler as the analogue Bethe–Salpeter equations, and they can be numerically solved with present-day computers. The only principal approximation, that is necessary to do in this approach is the truncation of the intermediate multi-particle states. But here, unlike to the Bethe–Salpeter equations,

one must cut down only the *on mass shell intermediate states*. In any case, for a self-consistent calculation of the two-body and the three-body reactions in the low- and intermediate-energy region, it is advisable to work out a scheme of a suppression mechanism of the transition of one off-mass-shell fermion into the on-mass-shell fermion+on-mass-shell boson which arise together with the transition amplitude into the three-fermion + boson states (see Figs. 3a, 3b, 3d and 3e).

## References

- [1] A. N. Kvinikhidze and B. Blankleider, Nucl. Phys. A **574** (1994) 488.
- [2] D. R. Phillips and I. R. Afnan, Ann. Phys. **240** (1995) 266; **247** (1996) 19.
- [3] R. G. Newton, *Scattering Theory of Waves and Particles*, Berlin, Springer-Verlag (1982).
- [4] M. L. Goldberger and M. Watson, *Collision Theory*, New York, John Wiley and Sons (1965).
- [5] J. D. Bjorken and S. D. Drell, *Relativistic Quantum Fields*, New York, McGraw-Hill (1965).
- [6] C. Itzykson and C. Zuber, *Quantum Field Theory*, New York, McGraw-Hill (1980).
- [7] F. Gross, *Relativistic Quantum Mechanics and Quantum Field Theory*, New York, John Wiley and Sons (1993).
- [8] A. I. Machavariani and A. Faessler, arXiv:nucl-th/0306040 2003, to be published in Ann. Phys.
- [9] V. De Alfaro, S. Fubini, G. Furlan and C. Rosseti, *Currents in Hadron Physics*, North-Holland, Amsterdam (1973).
- [10] M. K. Banerjee and J. B. Cammarata, Phys. Rev. C **17** (1978) 1125.
- [11] A. I. Machavariani, Sov. J. Part. Nucl. **24** (1993) 731.
- [12] A. I. Machavariani, A. J. Buchmann, Amand Faessler and G. A. Emelyanenko, Ann. Phys. **253** (1997) 149.
- [13] A. I. Machavariani, Phys. Lett. B **540** (2002) 81.
- [14] R. Haag, Phys. Rev. **112** (1958) 669; K. Nishijima, Phys. Rev. **111** (1958) 995; W. Zimmermann, Nuovo Cim. **10** (1958) 598; K. Huang and H. A. Weldon, Phys. Rev. D **11** (1975) 257.

RELATIVISTIČKA FORMULACIJA TEORIJE POLJA ZA  
TRODIMENZIJSKE JEDNADŽBE SUSTAVA TRI FERMIONA

Predlaže se nova vrsta relativističkih jednadžbi za sustave tri fermiona. Jednadžbe se izvode u okviru standardne teorije polja i  $S$  matrice u vremenski-uređenom trodimenzijskom obliku. Stoga su odgovarajuće relativističke kovarijantne jednadžbe od početka trodimenzijske, a nova formulacija nema neodređenosti koje se javljaju zbog sažimanja na tri dimenzije četiridimenzijskih Bethe–Salpeterovih jednadžbi. Rješenja novih jednadžbi automatski zadovoljavaju uvjete unitarnosti, a za leptone, te su jednadžbe egzaktno baždarno invarijantne, čak i nakon odreza mnogočestičnih ( $n > 3$ ) međustanja. Nadalje, oblik tih tročestičnih jednadžbi ne ovisi o odabiru Lagrangijana, i jednak za formulacije sa i bez kvarkovskih stupnjeva slobode. Efektivan se potencijal novih jednadžbi definira vršnim funkcijama s dvije čestice na ljusci mase. Naglašava se da se ULAZNE vršne funkcije mogu izvesti iz mjernih podataka.

Posebna se pažnja obraća usporedbi s Faddeevim jednadžbama. Za razliku od tih jednadžbi, nove tročestične jednadžbe su oblika Lippmann–Schwingerovih jednadžbi s povezanim potencijalom. Nadalje, mikroskopski potencijal novih jednadžbi sadrži doprinose sila tri tijela i mehanizma stvaranja (poništenja) vanjskih čestica. Analizira se struktura tročestičnih sila koje se javljaju u razmatranoj formulaciji u okviru teorije polja.